1.E.4: 2.N *Nuclear Physics* **A226** (1974) 326—346; © *North-Holland Publishing Co., Amsterdam*

INVESTIGATION OF THE 3.46 MeV ISOMERIC LEVEL OF ^{38}K WITH THE ^{24}Mg(^{16}O, pnγ)^{38}K REACTION

M. A. VAN DRIEL, H. H. EGGENHUISEN, J. A. J. HERMANS, D. BUCURESCU †, H. A. VAN RINSVELT †† and G. A. P. ENGELBERTINK

Fysisch Laboratorium, Rijksuniversiteit, Utrecht, The Netherlands

Received 26 March 1974

Abstract: The $\tau_{\frac{1}{2}} = 22\ \mu$s isomeric level of ^{38}K at an excitation energy of 3458.0±0.2 keV is strongly populated in the ^{24}Mg(^{16}O, pnγ)^{38}K reaction. Delayed γ-rays are studied with Ge(Li), Si(Li), and NaI detectors. Accurate excitation energies, branching ratios and lifetimes of levels involved in the decay of the isomeric state are determined. The isomeric level predominantly decays by a dipole transition of 38.03±0.03 keV with a total conversion coefficient of $\alpha_T = 0.42\pm0.15$. Mean lives of ^{38}K levels are measured with the recoil-distance method. The results are $\tau_m = 10.1\pm0.9$ ps, 1.41±0.14 ns and 101±15 ps for the levels at excitation energies of 0.46, 2.65 and 3.42 MeV, respectively. It is suggested that the $(1f_{\frac{7}{2}})^2$ structure of a low-lying $J^\pi = 7^+$ state in combination with the selection rules for γ-decay in a self-conjugate nucleus is responsible for the isomerism.

E NUCLEAR REACTIONS Mg+^{16}O, $E(^{16}O) = 36$, 38 MeV; measured delayed γ-rays, E_γ, I_γ, ICC; ^{38}K levels deduced E_x, branchings; measured recoil distance; ^{35}Cl, ^{38}Ar, ^{38}K levels deduced $T_{\frac{1}{2}}$. Natural targets.

1. Introduction

Positive parity states in nuclei at the end of the sd shell are expected to have admixtures of configurations consisting of excitation of an even number of particles to the fp shell. A clear example is e.g. the second excited state of ^{38}Ar at 3.38 MeV with $J^\pi = 0^+$, of which the configuration is predominantly [1]) $(sd)^{-4}(fp)^2$.

Recent shell-model calculations [2]) describe positive parity states in $A = 34$–38 nuclei with a complete set of (2s, 1d) basis states outside a closed ^{16}O core and account in this way for a large number of experimental observables. Excitation of an even number of particles from the sd to the fp shell is ignored in the calculations and the inherent limitations are discussed in terms of the existence of intruder states. The frequency of occurrence of low-lying intruder states would be an indication of the inadequacy of the model space used and from this point of view it is of interest to localize such states experimentally and to investigate their interplay with the sd shell states.

† Permanent address: Institute of Atomic Physics, P.O. Box 35, Bucharest, Rumania.
†† Permanent address: University of Florida, Gainesville, Florida, USA.

The existence of a $\tau_{\frac{1}{2}} \approx 23$ μs isomeric state excited in 24 MeV α-particle bombardment of Cl has first been reported by Ivanov *et al.* [3]). Delayed γ-rays of 0.042, 0.78, 2.73 and 3.54 MeV were observed with a 4 cm × 2.5 cm NaI crystal. The assignment to a particular nucleus, however, was not clear.

In a study of the reaction ^{40}Ca(d, $\alpha\gamma$)^{38}K, Hasper *et al.* [4]) noted that a weak peak in the α-particle singles spectrum corresponding to an excitation energy of about 3460 keV showed no coincidence with γ-rays. A level with a lifetime appreciably longer than 50 ns would be consistent with the data.

Recently, Iordăchescu *et al.* [5]) assigned the isomeric state with a half-life of $\tau_{\frac{1}{2}} = 22.1 \pm 0.7$ μs to ^{38}K and measured the g-factor with the time-differential spin precession method. The result of $g = 0.548 \pm 0.002$ is consistent with a pure $f^2_{\frac{7}{2}}$, $J^\pi = 7^+$ configuration.

Measurements with the ^{36}Ar(α, d)^{38}K reaction [6]) at $E_\alpha = 35$ MeV show a spectrum dominated by a state at 3445 ± 20 keV. Its deuteron angular distribution is similar to that of the ^{40}K(2.54 MeV) state populated strongly in the ^{38}Ar(α, d) reaction [6]) and to have known [7]) $J^\pi = 5$ or 7^+.

The present work with the ^{24}Mg(^{16}O, pnγ)^{38}K reaction gives excitation energies, branching ratios and lifetimes for the isomeric state and the levels involved in its decay. Preliminary results presented earlier [8]) are superseded by the present work.

2. Decay properties of the isomeric state

2.1. EXPERIMENTAL PROCEDURE

Self-supporting natural Mg targets with a thickness of about 1 mg/cm^2 are bombarded with a 38 MeV $^{16}O^{6+}$ beam of about 100 nA (electrical) intensity.

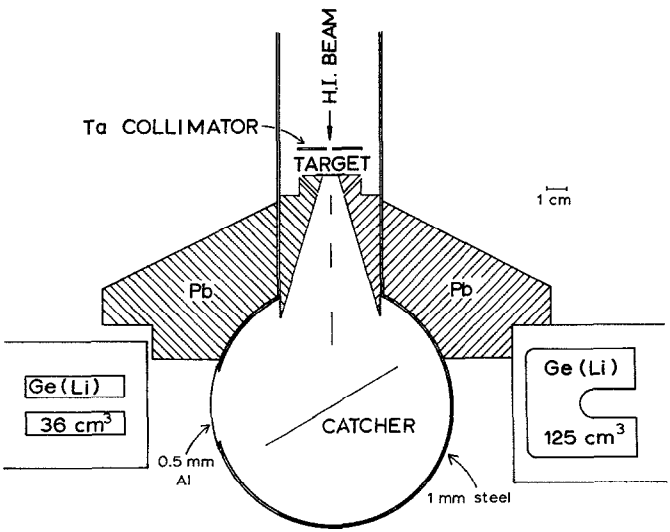

Fig. 1. Experimental set-up used to observe delayed γ-rays. The nuclei produced recoil from the target to a Ta or Cu catcher at a distance of 12 cm ($\approx$ 15 ns flight path).

The nuclei produced are allowed to recoil from the target to a Ta or Cu catcher at 12 cm distance ($\approx$ 15 ns flight path) and delayed γ-rays are studied with a 0.1 cm^3 Si(Li), 36 and 125 cm^3 Ge(Li) detectors and a 12.7 cm $\times$ 12.7 cm NaI crystal. The detectors are shielded from the direct radiation produced in the target by at least 10 cm Pb, which attenuates the intensity of 1 and 3 MeV γ-rays by factors of 2700 and 115, respectively. The experimental set-up is shown in fig. 1.

For γ-γ coincidence measurements, event-mode recording techniques were employed using a CDC 1700 computer and standard electronics.

2.2. RESULTS

2.2.1. Energies and intensities. A γ-ray singles spectrum recorded with the 36 cm^3 Ge(Li) detector in the set-up of fig. 1 is shown in fig. 2. A tantalum catcher was used.

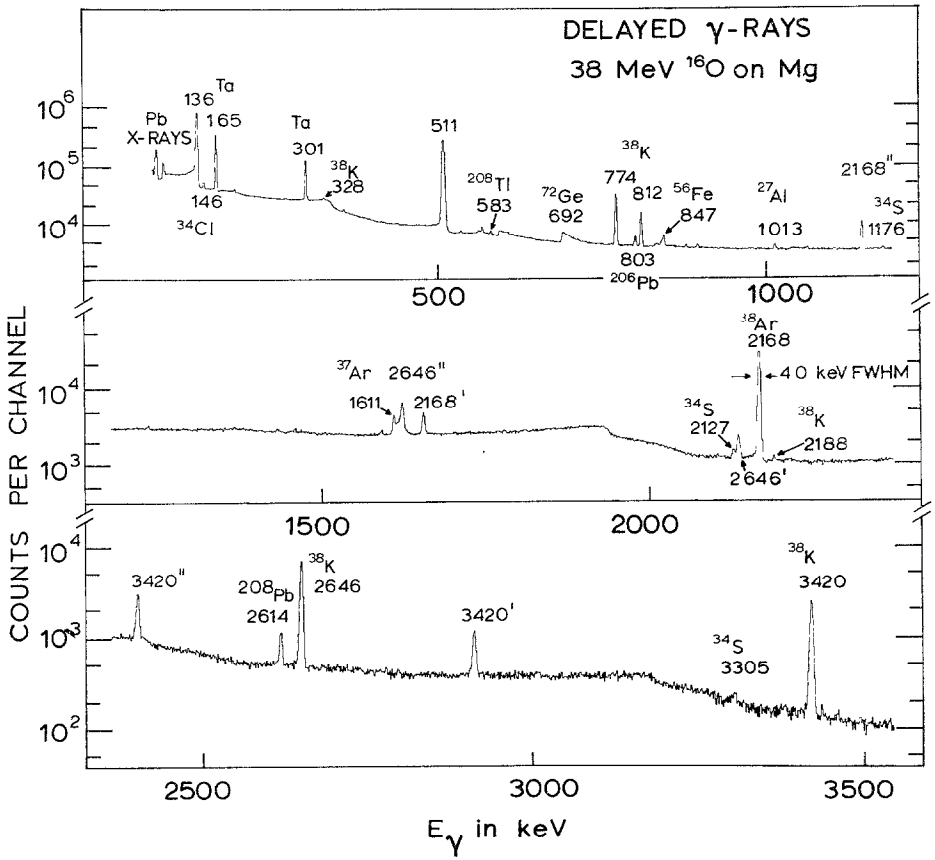

Fig. 2. A γ-ray singles spectrum taken with a 36 cm^3 Ge(Li) detector in the set-up of fig. 1. A self-supporting natural Mg target with a thickness of 900 $\mu g/cm^2$ is bombarded with a 38 MeV $^{16}O^{6+}$ beam of 80 nA (electrical). The peaks are labeled with the corresponding γ-ray energies in keV; primes and double primes indicate single-escape and double-escape peaks, respectively. A Ta catcher was used.

The γ-rays observed originate from (i) levels with a mean life longer than a few ns, e.g. isomers of β-decaying states; (ii) reactions of the ^{16}O beam with the material of the catcher (mainly the Coulomb excitation lines of ^{181}Ta are seen with energies of 136, 165 and 301 keV); (iii) (n, n'γ) reactions induced in the surrounding material, e.g. 692 and 835 keV from ^{72}Ge, 803 keV from ^{206}Pb, 847 keV from ^{56}Fe (goniometer table), 1014 keV from ^{27}Al (Ge(Li) hood) and 2614 keV from ^{208}Pb (lead shielding); (iv) room-background lines as 583 keV from ^{208}Tl and 1461 keV from ^{40}K. The strong peak at 2168 keV is the ^{38}Ar(1 → 0) transition following the β^+ decay of ^{38}K. The peaks labeled ^{34}Cl and ^{34}S are due to the reaction ^{24}Mg(^{16}O, pnα) ^{34}Cl(1)(β^+)^{34}S.

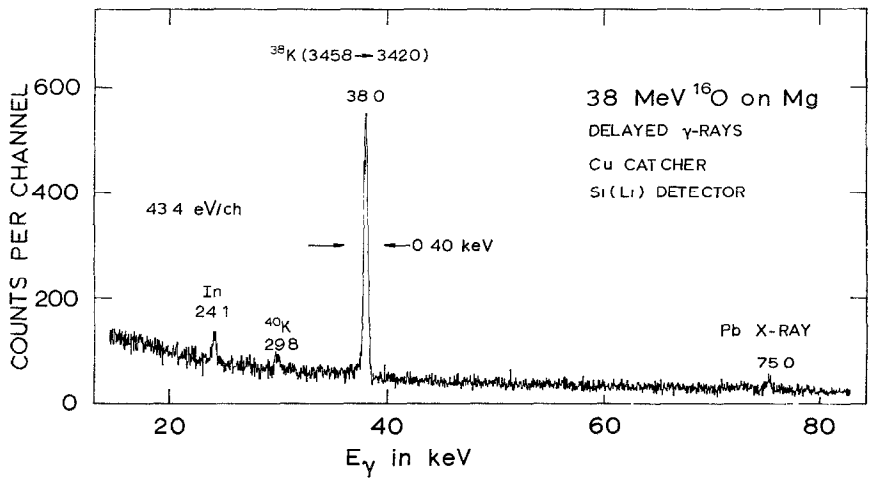

Fig. 3. A γ-ray singles spectrum taken with a 0.1 cm^3 Si(Li) detector in the set-up of fig. 1. A self-supporting natural Mg foil with a thickness of 1.5 mg/cm^2 is bombarded with a 38 MeV $^{16}O^{6+}$ beam of about 80 nA (electrical). The peaks are labeled with the corresponding γ-ray energies in keV. A Cu catcher was used.

A low-energy γ-ray singles spectrum recorded with the 0.1 cm^3 Si(Li) detector in the set-up of fig. 1 is shown in fig. 3. A Cu catcher was used instead of Ta to reduce the number of low-energy γ-rays due to reactions of the ^{16}O beam with the catcher material. The Ta and Cu K_{α_1} X-rays have energies of 57.5 and 8.05 keV, respectively. The spectrum is dominated by a 38.0 keV γ-ray and weak peaks are observed at 24.1 and 29.8 keV. A direct spectrum taken in another set-up with the Si(Li) detector at 1.5 cm from the target and at 90°, shows the peaks of fig. 3 with better statistics and subsequent energy measurements with sources of ^{182}Ta and ^{241}Am yield energies of 29.83±0.03 keV and 24.14±0.03 keV. The 29.8 keV line observed in fig. 3 should be the ^{40}K(1 → 0) transition formed via the ^{26}Mg(^{16}O, pnγ)^{40}K reaction. Its observation in the delayed spectrum would be consistent with the known energy (29.6±0.1 keV) and mean life (τ_m = 6.12±0.12 ns) [ref. ^{7})]. The 24.1 keV peak in fig. 3 is

TABLE 1

Delayed γ-ray transitions in ^{38}K observed from the bombardment of Mg with ^{16}O

Energy [a] (keV)	Assignment in ^{38}K ($E_i \rightarrow E_f$ in MeV)	Relative intensity
38.03±0.03	3.46 → 3.42	121 ±13
328.3 ±0.3	0.46 → 0.13	2.6± 0.4
773.9 ±0.2	3.42 → 2.65	100
811.9 ±0.2	3.46 → 2.65	39.5± 0.6
2187.4 ±0.5	2.65 → 0.46	1.7± 0.2
2646.1 ±0.2	2.65 → 0	140 ±5
3420.0 ±0.3	3.42 → 0	72 ± 3
3458	3.46 → 0	< 0.2

[a]) Recoil energy included.

interpreted as the intensity weighted sum of the K_{α_1} and K_{α_2} X-rays of In, a material used in the construction of the Si(Li) detector. In the above mentioned direct spectrum the weaker K'_{β_1} X-ray of In is also observed. The 24.1 and 29.8 keV peaks are not in coincidence with ^{38}K γ-rays (see subsect. 2.2.2).

The spectra of figs. 2 and 3 and similar ones taken under slightly different conditions result in the energies and intensities given in table 1. The energy of the 38.03±0.03 keV γ-ray is measured relative to the 31.735±0.001 [ref. [9])] γ-ray of ^{182}Ta with the mixed-source technique applied to a delayed Si(Li) spectrum. The energies of the other γ-rays in column 1 of table 1 are obtained from delayed spectra mixed with γ-rays from sources of ^{54}Mn, ^{56}Co, ^{137}Cs and ^{228}Th. The data are analysed with techniques similar to those described in ref. [10]).

The intensities of the peaks in the delayed spectra are obtained from measurements with both Ge(Li) detectors. Their efficiency calibration was determined with radioactive sources taped to the catcher in the same set-up as for the experiments. Sources of ^{56}Co [ref. [11])], ^{88}Y [ref. [12])], ^{133}Ba [ref. [13])], ^{182}Ta [ref. [9])] and ^{228}Th [ref. [14])] were used with the γ-ray intensities taken from the references indicated. The intensity ratio I(38 keV)/I(774 keV) is determined with the 36 cm^3 Ge(Li) detector, which has no n-type layer in front of the active volume of the Ge(Li) crystal (1 mm Ge has a transmission of only 4.3 % for 38 keV).

2.2.2. Assignment of the delayed γ-rays to ^{38}K. for the 2.65 MeV level the following results are obtained with the Mg+^{16}O reaction: E_x = 2646.1±0.2 keV, (98.8±0.2)% ground-state decay and τ_m = 1.41±0.14 ns (see sect. 3). Recent α-γ coincidence measurements with the ^{40}Ca(d, $\alpha\gamma$)^{38}K reaction [15]) result in E_x = 2646.3±0.7 keV, 100 % ground-state decay and τ_m > 12 ps. The agreement for excitation energy, decay and lifetime leads to the assumption that the two reactions excite the same level in ^{38}K. The presently observed 2.65 → 0.46 and 0.46 → 0.13 MeV transitions, involving well-known [7]) low-lying ^{38}K levels strengthen this assumption.

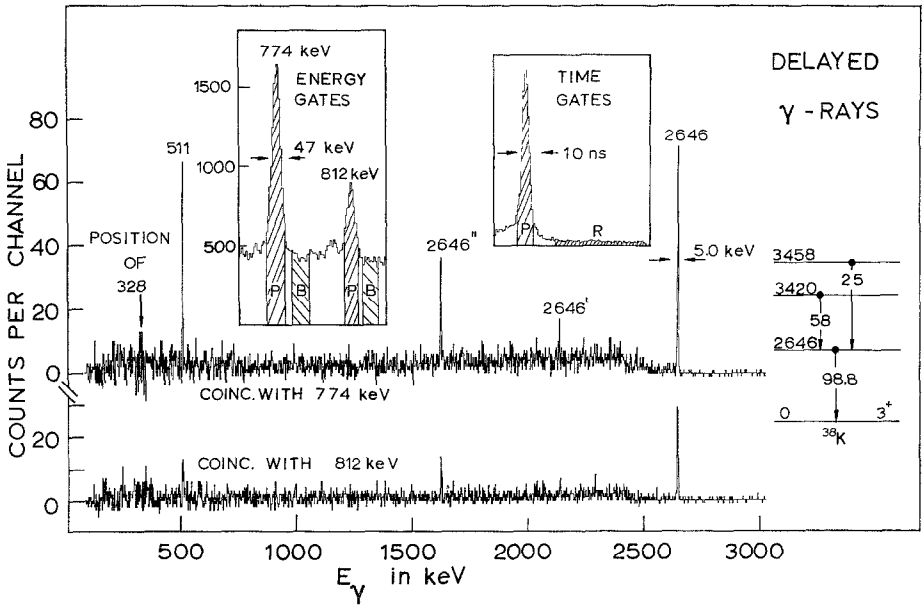

Fig. 4. Results of a Ge(Li)-Ge(Li) coincidence experiment with delayed γ-rays. Ge(Li) detectors of 36 and 125 cm^3 were used in the geometry of fig. 1. The two spectra shown are corrected for background and randoms with gates as indicated in the inserts. The peaks are labeled with the corresponding γ-ray energies in keV; primes and double primes indicate single-escape and double-escape peak, respectively.

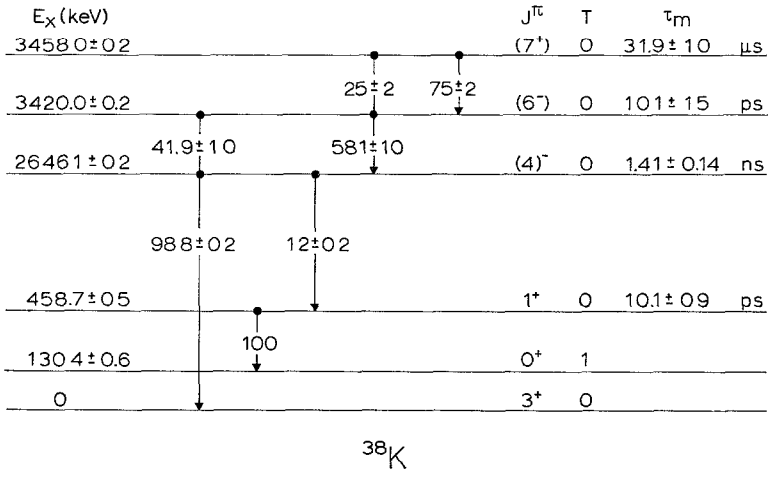

Fig. 5. Decay scheme of some ^{38}K levels. Detailed information is found in tables 2, 3 and 5. For T and J^π assignments, see subsects. 4.2 and 4.3, respectively. The J-values given in brackets are upper limits.

TABLE 2
Excitation energies (keV) of some ^{38}K levels

Present work	Ref. [15])	Ref. [7])
130.4±0.6	130.8±1.0	131±2
458.7±0.5	458.8±1.0	461± 2
2646.1±0.2	2646.3±0.7	2647± 2
3420.0±0.2	3418.9±2.1	
3458.0±0.2		(3470±20)

TABLE 3
Gamma-ray branching ratios [a]) of ^{38}K levels (E_x in MeV) from the ^{24}Mg(^{16}O, pnγ)^{38}K reaction

To [b]) \ From	2.65	3.42	3.46
0	98.8±0.2	41.9±1.0	<0.12 [d])
0.13	<0.4	<0.2	<0.2
0.46	1.2±0.2	<0.3	<0.3
1.70	<0.2	<0.4	<0.4
2.40	<0.3	<0.4	<0.3
2.61	<1.3	<2.3 [c])	<0.7 [e])
2.65		58.1±1.0	25±2 [f])
2.83		<0.2	<0.3
2.87		<0.3	<0.3
2.99		<0.3	<0.3
3.05		<0.9	<0.3
3.32		<0.2	<0.4
3.34		<0.3	<0.3
3.42			75±2 [f])

[a]) The upper limits are given at the 95% confidence level.
[b]) Taken from ref. [15]), except for the 0.13, 0.46, 2.65 and 3.42 MeV levels.
[c]) From a Si(Li)-Ge(Li) coincidence measurement.
[d]) Measured at a target-detector distance of 28 cm to reduce summing effects; see fig. 6 and text.
[e]) From a NaI-Ge(Li) coincidence measurement.
[f]) With the internal conversion taken into account, the transition branching ratios are (18.7±0.4)% and (81.3±0.4)%.

Results of a γ-γ coincidence experiment with the delayed γ-rays are presented in fig. 4. Ge(Li) detectors of 36 and 125 cm^3 were used in the geometry shown in fig. 1. The data, corrected for background (gate B) and randoms (gate R) show clearly the 774 and 812 keV γ-rays coincident with the 2646 keV γ-ray.

Additional evidence for the present assignment to ^{38}K is found from the results for the 3.42 MeV level. The Mg+^{16}O reaction yields E_x = 3420.0±0.2 keV and branches of (58.1±1.0)% to the 2.65 MeV level and (41.9±1.0)% to the ground state, while the results of the ^{40}Ca(d, $\alpha\gamma$)^{38}K reaction [4,15]) are 3419±2 keV, (55±10)% and (45±10)%, respectively.

The recoil-corrected γ-ray energies of table 1 lead to the excitation energies given in table 2. The branching ratios obtained from the γ-ray intensities are given in table 3 and the resulting decay scheme is shown in fig. 5. Since the lifetimes of the 0.46, 2.65 and 3.42 MeV levels (see sect. 3) are short compared to the flightpath used, the γ-ray intensities in table 1 are due to the decay of the isomeric level only. The following internal checks on energies and intensities are seen to be consistent with zero:

$$E(812)-E(774)-E(38) = -0.06\pm0.09 \text{ keV};$$

$$E(3420)-E(2646)-E(774) = 0.0\pm0.3 \text{ keV};$$

$$I(2646)+I(2188)-I(774)-I(812) = (2\pm5)\%;$$

$$I(328)-I(2188) = (0.9\pm0.5)\%.$$

2.2.3. Upper limits on branching ratios. The upper limits on branching ratios in table 3 are given at the 95 % confidence level. They are mainly determined from delayed γ-ray spectra taken with the 125 cm^3 Ge(Li) detector and are equal to $4\sqrt{N \cdot \text{FWHM}}$, where N denotes the spectrum intensity in a particular region and values for FWHM (full width at half maximum) were estimated from the widths of neighbouring peaks. This particular limit corresponds to two standard deviations in a result not significantly different from zero.

In some cases where a possible transition in the singles spectra was hidden under a contaminant peak, the upper limit given is obtained from γ-γ coincidence measurements.

For the 3.46 → 2.61 MeV transition a NaI-Ge(Li) coincidence measurement was performed with a gate between 2450 and 2850 keV on the NaI spectrum. In the resulting Ge(Li) spectrum only the 774 and 812 keV peaks were observed. The extracted upper limit for the 3.46 → 2.61 MeV transition is given in table 3.

For the 3.42 → 2.61 MeV transition a Si(Li)-Ge(Li) coincidence measurement was performed. The Ge(Li) spectrum in coincidence with 38 keV shows in the region 750–850 keV only the 774 keV peak. The extracted upper limit for the 3.42 → 2.61 MeV transition is given in table 3.

The upper limit for the decay of the isomeric level to the ground state is obtained from a delayed spectrum measured with the 125 cm^3 Ge(Li) detector at 28 cm distance from the target to reduce the summing effects from the cascades 3.46 → 3.42 → 0 and 3.46 → 2.65 → 0 MeV. In addition, the summing due to the 3.46 → 3.42 → 0 MeV cascade was eliminated by shielding the Ge(Li) detector with 4 mm Pb. The result obtained is shown in fig. 6 and the extracted upper limit is given in table 3. For an E4 transition (see discussion) the upper limit would correspond to a strength of only 3.2×10^{-3} W.u.

2.2.4. Conversion coefficient of the 38 keV γ-ray. From the theoretical conversion coefficients given in table 4, it follows that the low-energy 38 keV γ-ray is expected to be converted appreciably, in spite of the low value of $Z = 19$. The theoretical con-

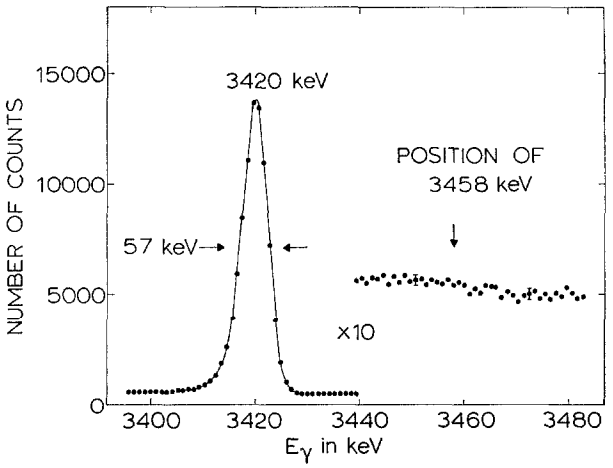

Fig. 6. Delayed γ-ray spectrum measured with the 125 cm^3 Ge(Li) detector at a distance of 28 cm from the target. The detector was shielded with 4 mm Pb. The resulting upper limit for the ground-state transition of the isomeric level is given in table 3, see subsect. 2.2.3.

TABLE 4

Conversion coefficient α_T for the 38.0 keV ray in ^{38}K

Multipolarity	α_T	
	theoretical [a])	experimental
E1	0.39	0.42±0.15
M1	0.13	
E2	10.4	

[a]) Extrapolated from the tables of Rose [16]), see text.

version coefficients are calculated by extrapolation (on a double logarithmic plot) of the values given by Rose [16]) for $Z = 25$ and higher.

The experimental total conversion coefficient α_T is determined from the intensities of the 38, 774 and 3420 keV γ-rays given in table 1, namely $\alpha_T+1 = [I(774)+I(3420)]/I(38)$.

The result is $\alpha_T = 0.42\pm0.15$. A comparison with the theoretical conversion coefficients in table 4 yields the conclusion that the 38 keV transition cannot have pure E2 character. The mean life and branching ratio alone would give for the E2 possibility a strength of 24 W.u., which is unlikely but not impossible.

3. Recoil-distance lifetime measurements

The ^{38}K states with excitation energies of 0.46, 2.65 and 3.42 MeV are populated in the ^{24}Mg(^{16}O, pnγ)^{38}K reaction and the recoil-distance method was used to measure the lifetimes.

Since the bombardment of Mg with ^{16}O produces a number of final nuclei simultaneously, results are obtained concurrently for the ^{35}Cl(3.16 MeV), ^{38}Ar(4.59 MeV) and ^{38}Ar(6.41 MeV) states.

3.1. EXPERIMENTAL DETAILS

The plunger apparatus used has a range of 10 cm and a better than 4 μm accuracy for 0–1000 μm. The zero distance is measured electrically before and after each run.

The 20–40 nA (electrical) $^{16}O^{6+}$ beam with an energy of 36 MeV is focussed through a collimator to a 2 mm diameter beam spot on the stretched target foil, of which the position is fixed during the measurement. The recoiling nuclei and the beam are stopped in a thick circular Au stop of 7.5 cm diameter.

The targets consisted of about 100 and 300 μg/cm^2 Mg on 1 μm thick Ni, with the target material on the down-stream side. The energy loss of the beam in the Ni foil is about 3.7 MeV.

The γ-rays were detected by means of a 125 cm^3 Ge(Li) detector placed at 0° with respect to the beam and at a distance of 6.8 or 11.8 cm from the target foil.

3.2. ANALYSIS

The analysis closely follows the methods outlined in refs. [17,18]). For an ensemble of excited nuclei, travelling with a constant velocity $v = \beta c$ over the recoil distance D, the mean life τ of the state is derived from the exponential decay curve of the stopped peak

$$R(D) = I_0/(I_0+I_s) = \exp(-D/v\tau). \quad (1)$$

Here, I_0 and I_s denote the intensities of the stopped and shifted peaks, respectively.

3.2.1. Determination of $R(D)$. In extracting the ratio $R(D)$ from the experimentally observed areas A_0 and A_s of the stopped and shifted peaks, the latter area is corrected for two effects.

(i) The detection efficiency for the shifted (higher energy) peak is smaller than for the unshifted peak. This correction is taken into account by multiplying A_s with the factor $(1+\beta)$, which corresponds to a $1/E_\gamma$ dependence for the efficiency.

(ii) Due to the motion of the recoiling nuclei, the solid angle of the Ge(Li) detector is larger for the shifted peak than for the stopped peak. This correction is accounted for by multiplying A_s with the factor $(1-\beta)/(1+\beta)$. So the combined effect of the efficiency and Lorentz correction results in

$$R(D) = A_0/\{A_0+(1-\beta)A_s\}.$$

Reactions like (^{16}O, pn) generally yield a large velocity spread for the recoiling nuclei so that the shifted peaks are considerably Doppler broadened. Especially for the higher-energy γ-rays it is then difficult to determine A_s with the same precision as A_0. Therefore some decay curves are normalized by means of the stopped peaks of γ-rays de-exciting long-lived states, which are populated simultaneously with the

levels under investigation. Examples are the transitions ^{38}K(3.46 → 2.65 MeV) with $\tau_m = 31.9 \pm 1.0$ μs [ref. [5])] and ^{37}Ar(1.61 → 0) MeV with $\tau_m = 6.3 \pm 0.2$ ns [ref. [7])]. The latter is used only for short distances, where the effect of its finite lifetime is still small and calculable with sufficient precision. The analysis with $R'(D) = A_0/A_n$ is also advantageous if the plunger distances are not negligibly small compared with the target-detector distance, such that solid-angle corrections depending on the origin of the radiation have to be considered. It should be noted, however, that for peaks A_0 and A_n, very different in energy, solid-angle effects due to the point of detection in the Ge(Li) detector have also to be taken into account.

3.2.2. Effect of the recoil-velocity distribution. The energy straggling of the oxygen beam in the Ni backing, the kinematics of the compound-nucleus reaction with two outgoing secondary particles and the straggling of the recoils in the target produce a recoil-velocity distribution of considerable width.

For the ^{24}Mg(^{16}O, pn)^{38}K(0.46 MeV) reaction at 31 MeV bombarding energy, the kinematical extreme situations of emission of a deuteron at 0°, 180° and 90° c.m., result e.g. in a minimum recoil velocity of $\beta_{min} = 1.92$ %, a maximum recoil velocity of $\beta_{max} = 3.24$ % and a maximum recoil half-angle of 14.3°, respectively.

The effect of the recoil-velocity distribution f on $R(D)$ has been considered by Jones *et al.* [17]). Its influence is expressed by writing

$$R(D) = e^{-D/\bar{v}\tau}\psi(f). \tag{2}$$

The function $\psi(f)$ is expanded in terms of the moments of the velocity distribution around the mean velocity $\bar{v}$ and has the form

$$\psi(f) = 1 + \sum_{n=2}^{\infty} a_n M_n(f). \tag{3}$$

Here $M_n(f)$ is the nth moment of the velocity distribution f and the a_n are expansion coefficients. These expansion coefficients have the form of polynomials of degree n in $D/\bar{v}\tau$ given by

$$a_n = \sum_{k=0}^{n-1} \left(\frac{-D}{\bar{v}\tau}\right)^{n-k} \frac{(n-1)!}{(n-k)!(n-k-1)!k!}. \tag{4}$$

In fig. 7 a numerical evaluation of $\psi(f)$ is presented as a function of $D/\bar{v}\tau$. The velocity distribution is taken to be a parabola, characterized by the parameter W, defined as $W \equiv \mathrm{FWHM}/E_\gamma(\bar{v}/c)\cos\theta$ with FWHM the full width at half maximum of the velocity distribution. Fig. 7 shows that $\psi(f)$ deviates considerably from unity for broad velocity distributions and large values of $D/\bar{v}\tau$. However, for distances up to $D/\bar{v}\tau = 2$ and $W < 1.0$ the deviation of $\psi(f)$ from unity is less than 5 %. In a measurement of the lifetime of the ^{35}Cl(3.16 MeV) state with the ^{24}Mg(^{16}O, pα)^{35}Cl reaction e.g. a value of $W = 1.1$ is encountered.

In the analysis of the data the actual velocity distribution is extracted from the shifted peak in spectra taken at large distances ($D/\bar{v}\tau > 3$), because at small distances

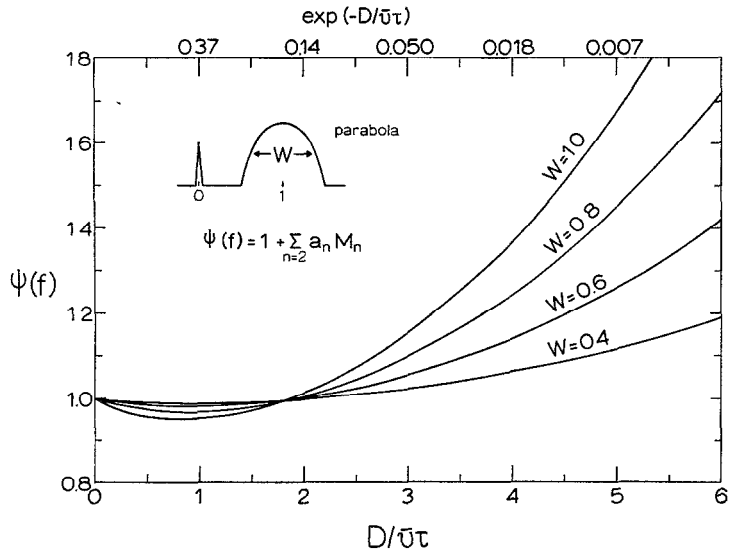

Fig. 7. The velocity-distribution correction function $\psi(f)$ as a function of $D/\bar{v}\tau$. The velocity distribution f is taken to be a parabola, characterized by the parameter W as shown in the insert, see subsect. 3.2.2.

the observed distribution is deformed by the presence of the stop. After applying efficiency, Lorentz and detector-smearing corrections to the observed shifted peak, the particular velocity distribution f is parametrized in a simple way and $\psi(f)$ is calculated from eq. (3). The quantity $R(D)/\psi(f)$ is finally fitted with an exponential to obtain $D_m = \bar{v}\tau$.

3.2.3. Determination of $\bar{v}$. The energy difference ΔE between the centroids of stopped and shifted peak of the γ-ray with energy E is determined from the spectra taken at larger separation distances and $\bar{v} = \beta c$ is calculated from the second order Doppler shift equation

$$\frac{\Delta E}{E} = \beta \overline{\cos\theta} + \beta^2(\overline{\cos^2\theta} - \tfrac{1}{2}). \tag{5}$$

The terms $\overline{\cos\theta}$ and $\overline{\cos^2\theta}$ have to be evaluated over the solid angle of the Ge(Li) detector, taking its directional efficiency and the γ-ray angular distribution into account. For the present geometry ($\theta_\gamma = 0°$ and L cm distance between target and detector) $\cos\theta$ varies between 1.000 and 0.974 for $L = 11.8$ cm and between 1.000 and 0.928 for $L = 6.8$ cm. Neglect of angular distribution effects (a 7 % variation in the argument of $P_2(\cos\theta)$ induces a 6 % variation in the angular distribution $W(\theta) = 1 + A_2 P_2(\cos\theta)$ for $A_2 = 0.3$) reduces eq. (5) to

$$\frac{\Delta E}{E} = (1-\delta)\beta + (\tfrac{1}{2} - 2\delta)\beta^2. \tag{6}$$

The quantity δ amounts to 0.009 and 0.024 for $L = 11.8$ cm and 6.8 cm, respectively. The results for $\beta = \bar{v}/c$ given in table 5 are calculated from eq. (6).

TABLE 5
Survey of recoil distance lifetime results

Nucleus	State (MeV)	Transition $E_i \rightarrow E_f$ (MeV)	$\bar{v}/c$ (%)	τ_m (ps)	Adopted τ_m (ps)
^{38}K	0.46	0.46 → 0.13	2.29±0.10	10.1± 0.9	10.1± 0.9
	2.65	2.65 → 0	2.30±0.04	1430 ±170	1410 ±140
			1.90±0.04	1360 ±230	
	3.42	3.42 → 0	2.30±0.04	97 ± 17	101 ± 15
			1.90±0.04	115 ± 30	
^{35}Cl	3.16	3.16 → 0	2.22±0.04	43 ± 2	42 ± 2
			1.90±0.04	41 ± 2	
^{38}Ar	4.59	4.48 → 3.81	2.15±0.10	196 ± 10	196 ± 10
	6.41	6.41 → 4.59	2.15±0.10	< 3	< 3 [a])

[a]) The result of a DSA experiment is $\tau_m = 1.5 \pm 0.4$ ps (see text).

3.3. RESULTS

3.3.1. ^{38}K*(0.46 MeV)*. The 0.46 MeV level only decays to the 0.13 MeV level and the upper limit for the ground-state decay is 1 % [ref. [19])]. The shifted peak of the 328 keV γ-ray is close to the Compton edge of the 511 keV annihilation peak, which mainly stems from the β^+ decay of ^{38}K(0) and ^{38}K(1).

To facilitate the analysis, the annihilation peak and its Compton structure is removed from the spectra by subtracting a fraction of a spectrum obtained with a ^{22}Na source in the same plunger geometry. The fraction subtracted was about 5 % of the intensity of the ^{22}Na spectrum, so that statistical errors introduced by the subtraction are negligible. The data (after subtraction) are shown in fig. 8. The target was about 100 μg/cm^2 thick and the Ge(Li) detector was at 6.8 cm distance from the target.

The ratios $R(D) = I_0/(I_0+I_s)$ are shown in fig. 9. The alphabetical order indicates the time ordening of the data points. Because we have $W = 0.25$ and $D/\bar{v}\tau < 3$, the deviation of $\psi(f)$ from unity, less than 0.8 %, can be neglected. The constant background in fig. 9 is due to feeding from the long-lived levels at 2.65 and 3.46 MeV (see fig. 5) and does not originate from target material on the stopper surface as is shown e.g. by data taken in the same run pertaining to the 3.16 → 0 MeV transition in ^{35}Cl.

A fit of $\exp(-D/\bar{v}\tau)+$constant to the data points yields $D_m = 69 \pm 4$ μm, with the pre-alignment zero found to be at $D_0 = 3 \pm 2$ μm. A fit to $R'(D) = A_0/A_n$ with A_0 equal to the area of the stopped peak of the 328 keV γ-ray and A_n the area of the stopped peak of the 1.61 → 0 MeV transition in ^{37}Ar gives $D_m = 72 \pm 6$ μm. The adopted value of $D_m = 70 \pm 4$ μm leads, in combination with $\bar{v}/c = (2.29 \pm 0.10)$%, to the mean life of $\tau_m = 10.1 \pm 0.9$ ps given in table 5.

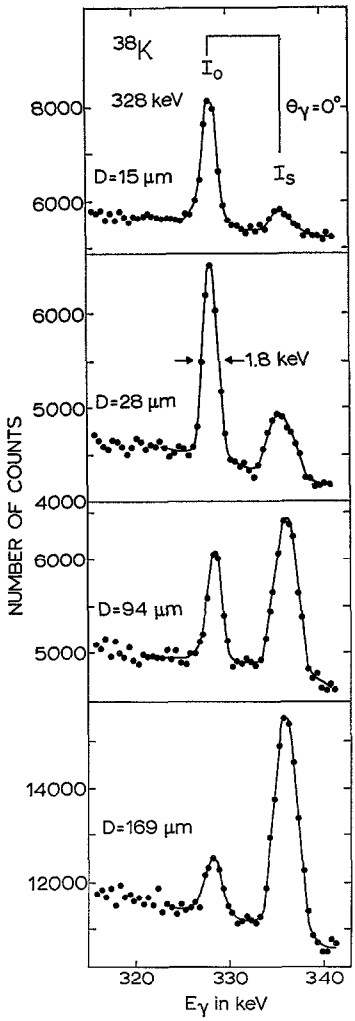

Fig. 8. The recoil-distance data for the 0.46 → 0.13 MeV transition in ^{38}K for target-stopper distances of 15, 28, 94 and 169 μm. See subsect. 3.3.1.

3.3.2. $^{38}K(3.42\ MeV)$. The data in fig. 10 show that at $E(^{16}O) = 36$ MeV the fast feeding (direct via particles or indirect via short-lived levels) of ^{38}K(3.42 MeV) is about one-third of the total feeding. The strong excitation via the isomeric level is responsible for the constant background and limits the accuracy in the lifetime result because $R'(D)$ changes by less than a factor of two. The ratio $R'(D)$ represents $A_0/A_n\psi(f)$ where A_n is the area of the stopped peak of the 1.61 → 0 MeV transition in ^{37}Ar, corrected for its own decay (see subsect. 3.2.1). The results of two runs with the Ge(Li) detector at 11.8 cm distance from the target are given in table 5.

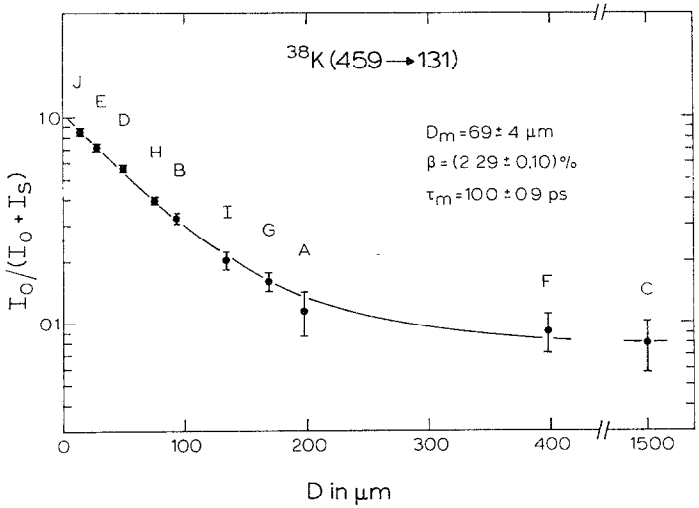

Fig. 9. The experimental ratios $I_0/(I_0+I_s)$ plotted as a function of target-stopper distance D for the 0.46 → 0.13 MeV transition in ^{38}K. The alphabetical order indicates the time ordening of the data points. The solid line is a fit of $\exp(-D/\bar{v}\tau)$+constant to the data points and yields $D_m = 69 \pm 4\,\mu$m.

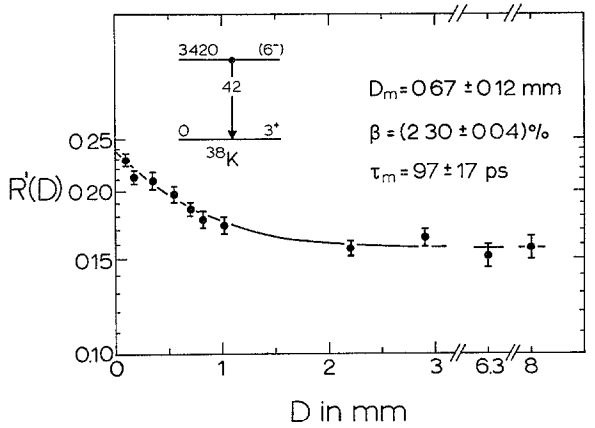

Fig. 10. The experimental ratios $R'(D)$ given as a function of the target-stopper distance D for the 3.42 → 0 MeV transition in ^{38}K. The ratio $R'(D)$ represents $A_0/A_n\,\psi(f)$ where A_n is the area of the stopped peak of the 1.61 → 0 MeV transition in ^{37}Ar, corrected for its own decay. The solid line is a fit of $\exp(-D/\bar{v}\tau)$+constant to the data points and yields $D_m = 0.67 \pm 0.12$ mm.

3.3.3. $^{38}K(2.65\,MeV)$. The data in fig. 11 show that the fast feeding of the ^{38}K(2.65 MeV) state is about one-half of the total feeding. The ratio $R'(D)$ represents the quantity $A_0/A_n\psi(f)$ with A_0 the area of the stopped peak of the 2646 keV γ-ray and A_n the area of the stopped peak of the 3420 keV γ-ray. In fig. 10 is shown that for the data points with $D > 2.0$ mm the stopped peak of the 3420 keV γ-ray is only due

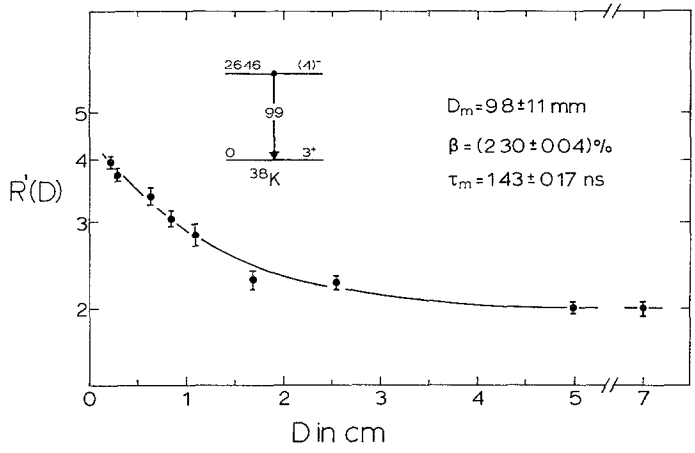

Fig. 11. The experimental ratios $R'(D)$ plotted as a function of the target-stopper distance D for the 2.65 → 0 MeV transition in ^{38}K. The ratio $R'(D)$ represents the quantity $A_0/A_n\ \psi(f)$ with A_0 the area of the stopped peak of the 2646 keV γ-ray and A_n the area of the stopped peak of the 3420 keV γ-ray. The solid line is a fit of $\exp(-D/\bar{v}\tau)$+constant to the data points and yields $D_m = 9.8 \pm 1.1$ mm.

to the isomeric feeding and therefore suitable for normalization. Also the difference in energy with the 2646 keV γ-ray is small which is important in view of the large variation in D compared to the 11.8 cm distance between target and Ge(Li) detector.

For separation distances with $D < 3.0$ mm the stopped peak of the 2646 keV γ-ray is distorted by the single-escape peak of the strong 3163 keV γ-ray. The correct 2646 keV area is obtained by determining the total area (3163 keV single-escape peak included) and subtracting a fraction of the 3163 keV full-energy peak. The ratio of the single-escape to full-energy peak for this detector at $E_\gamma = 3163$ keV is determined as 0.303 ± 0.014 from a ^{56}Co spectrum taken in the same geometry. The results of two runs are given in table 5.

3.3.4. ^{35}*Cl(3.16 MeV).* The level is populated strongly in the ^{24}Mg(^{16}O, p$\alpha\gamma$)^{35}Cl reaction and the decay of the stopped peak can be followed over a factor of about 60. The velocity distribution is quite broad ($W = 1.1$) and $\psi(f)$ deviates considerably from unity for the large distances ($D/D_m \approx 8$) involved. Neglect of the velocity distribution ($\psi(f) \equiv 1$ for all D) would result in an increase of 7 % for the mean life obtained presently. Also the χ^2 of the fit would deteriorate from 1.3 to 2.3.

Since the statistical error in this measurement is quite small (about 3 % for τ_m) the influence of possible de-orientation effects should be considered before an overall error is assigned. To check for these effects different γ-rays are used for the normalizing area A_n, namely the stopped peak of the ^{37}Ar (1.61 → 0 MeV) transition and the sum of the stopped and shifted peak of the ^{35}Cl(3.16 → 0 MeV) transition. Results obtained in this way differ by about 3 % and an overall error of 5 % is adopted to encompass these effects. Results of two runs with different velocities are given in table 5.

TABLE 6
Comparison of measured lifetimes with previous results

Nucleus	E_x (MeV)	τ_m (ps) present	τ_m (ps) previous	Ref.
^{38}K	0.46	10.1± 0.9	740 ±160	[19]
			> 4	[15]
	2.65	1410 ±140	> 12	[15]
	3.42	101 ± 15		
^{35}Cl	3.16	42 ± 2	42 ± 3	[20]
			39.4± 4.5	[21]
			53 ± 6	[22]
			37 ± 4	[23]
			60 ± 7	[24]
^{38}Ar	4.59	196 ± 10	181 ± 13	[25]
			172 ± 8	[26]
			226 ± 21	[27]
			196 ± 10	[28]
			189 ± 36	[29]
			194 ± 11	[21]
	6.41	1.5± 0.4		

3.3.5. ^{38}Ar *(4.59 MeV).* This level is populated in the ^{24}Mg(^{16}O, 2pγ)^{38}Ar reaction and the decay of the stopped peak of the 4.48 → 3.81 MeV transition results in the lifetime given in table 5.

3.3.6. ^{38}Ar *(6.41 MeV).* The excitation energy of this level was found to be 6408.2±0.3 keV. It exclusively decays with a 1822.4±0.2 keV γ-ray to the 4.59 MeV, $J^\pi = 5^-$ level. The recoil-distance measurement yields an upper limit of 3 ps.

Line-shape measurements with the DSA method with the ^{24}Mg(^{16}O, 2pγ)^{38}Ar and ^{27}Al(^{16}O, p$\alpha\gamma$)^{38}Ar reactions and Au as slowing-down material result in $\tau_m = 1.5 \pm 0.4$ ps. The targets consisted of about 100 μg/cm^2 Mg or Al on a 30 μm thick Au backing and the spectra were taken at $\theta_\gamma = 70°$.

A comparison between present and previous results is given in table 6.

4. Discussion

4.1. ANALOGOUS β- AND γ-TRANSITIONS

The relation between the $\Delta T = 1$, M1 transition probability and the *ft* value of the corresponding Gamow-Teller β-decay for ^{38}Ca($J^\pi = 0^+$, $T = 1$)(β^+)^{38}K($J^\pi = 1^+$, $T = 0$) is given by [see e.g. ref. [31])]

$$(ft)_{GT}(\text{in sec})|M(M1)|^2_{up}(\text{in W.u.}) = 5850 \left\{1 + 0.2125 \frac{\langle f||l\tau||i\rangle}{\langle f||\sigma\tau||i\rangle}\right\}^2. \qquad (7)$$

TABLE 7
Analogous β- and γ-transitions

^{38}K(E_x) [a] (MeV)	E_γ (keV)	τ_m	log ft [d] ^{38}Ca(β^+)^{38}K(E_x)	$\{1+0.2125\,A\}^2$	A [e]
0.46	328	10.1 $\pm$ 0.9 ps [b]	> 4.77	> 0.29	> -2.2 or < -7.2
1.70	1568	60 $\pm$15 fs [c]	3.30 ± 0.08	0.015 ± 0.004	-4.1 ± 0.1 or -5.3 ± 0.1
3.34	3212	< 55 fs [a]	3.90 ± 0.12	> 0.0077	> -4.3 or < -5.1

[a]) Ref. [15]).
[b]) Present work.
[c]) Refs. [15, 19]).
[d]) Ref. [30]).
[e]) $A \equiv \langle f||l\tau||i\rangle / \langle f||\sigma\tau||i\rangle$, see text.

Here i and f refer to initial and final state populated in the β^+ decay. The $J^\pi = 0^+$ and 1^+ states in ^{38}K are connected by a $\Delta T = 1$, pure M1 transition with $|M(\mathrm{M1})|^2_{\mathrm{up}} = \frac{1}{3}|M(\mathrm{M1})|^2_{\mathrm{down}} = 10.4/\tau_m E_\gamma^3$ with τ_m the mean life of the $J^\pi = 1^+$ state in fs and E_γ the γ-ray energy in MeV. The reduced matrix elements are reduced both with respect to angular momentum and to isospin.

The strengths of such analogous transitions give in combination with eq. (7) information about the amplitude and phase of the ratio $A \equiv \langle f||l\tau||i\rangle / \langle f||\sigma\tau||i\rangle$.

In the β^+ decay of ^{38}Ca(0) three ^{38}K levels with $J^\pi = 1^+$, $T = 0$ and excitation energies of 0.46, 1.70 and 3.34 MeV are populated. Their γ-decay [4, 7]) proceeds 100 % to the $J^\pi = 0^+$, $T = 1$ level at 0.13 MeV. Results for A given in table 7 show that for the 1.70 MeV level the ratio A is about -5. The importance of the orbital part is shown by the near cancellation of the quantity between brackets. For the other two levels only limits for A are obtained, due to the missing experimental information on the β^+ decay or on the lifetime.

4.2. ISOBARIC-SPIN ASSIGNMENTS

The ^{38}K analogues of the ^{38}Ar(0 MeV, $J^\pi = 0^+$, $T = 1$) and ^{38}Ar(2.17 MeV, $J^\pi = 2^+$, $T = 1$) levels are well established [7]) and have excitation energies of 0.13 and 2.40 MeV in ^{38}K, respectively. In a recent high-resolution study [32]) of the ^{40}Ca(d, α)^{38}K reaction with a spectrograph at $E_d = 10$–16 MeV these two levels are not or weakly populated, in agreement with the isospins involved.

The ^{38}K analogue of the second excited ^{38}Ar state, ^{38}Ar(3.38 MeV, $J^\pi = 0^+$, $T = 1$), is then expected at about $E_x = 3.6$ MeV in ^{38}K. In principle, both the 3.42 and the 3.46 MeV level could qualify.

However, the restriction for the 3.42 $\rightarrow$ 0 MeV transition given in table 8 excludes $J^\pi = 0^+$ for the 3.42 MeV level. In the above mentioned high-resolution study of the ^{40}Ca(d, α)^{38}K reaction the 3.42 and 3.46 MeV levels are quite well populated so that a $T = 1$ assignment is excluded. The resulting $T = 0$ assignments to the 2.65, 3.42 and 3.46 MeV levels are given in fig. 5.

TABLE 8

Radiative widths and electromagnetic transition strengths in ^{38}K

$E_{xi} \rightarrow E_{xf}$ [a] (MeV)	Partial Γ_γ [b] (eV)	Transition strength (W.u.)						Restrictions on J and π
		E1	M1	E2	M2	E3	M3	
0.46 → 0.13	6.5×10^{-5}		0.089					
2.65 → 0	4.6×10^{-7}	3.3×10^{-8}	1.2×10^{-6}	5.9×10^{-4}	2.2×10^{-2}	16	590	$\Delta J \leqq 3$, no M3
2.65 → 0.46	5.6×10^{-9}	7.0×10^{-10}	2.5×10^{-8}	1.8×10^{-5}	6.7×10^{-4}	0.73	27	$\Delta J \leqq 3$, no M3
3.42 → 0	2.7×10^{-6}	8.8×10^{-8}	3.2×10^{-6}	9.3×10^{-4}	3.4×10^{-2}	15	560	$\Delta J \leqq 3$, no M3
3.42 → 2.65	3.8×10^{-6}	1.1×10^{-5}	4.0×10^{-4}	2.2	83			$\Delta J \leqq 2$, no M2
3.46 → 2.65	3.9×10^{-12} [c]	9.4×10^{-12}	3.5×10^{-10}	1.8×10^{-6}	6.5×10^{-5}	0.50	18	$\Delta J \leqq 3$, no M3
3.46 → 3.42	1.2×10^{-11} [c]	2.8×10^{-7}	1.0×10^{-5}	24	880			$\Delta J \leqq 1$ [d]

[a]) All transitions have $\Delta T = 0$, with exception of the 0.46 → 0.13 MeV transition (see subsect. 3.4.2).

[b]) Computed from the branching ratios of table 3 and the mean lives in table 5.

[c]) Total conversion coefficient $\alpha_T = 0.42 \pm 0.15$ taken into account.

[d]) The observed total conversion coefficient limits the 38 keV transition to dipole radiation (see subsect. 2.2.4).

4.3. SPIN-PARITY RESTRICTIONS

The branching ratios and mean lives summarized in tables 3 and 5, respectively, lead to the radiative widths and electromagnetic transition strengths given in table 8. The transitions take place between levels of a self-conjugate nucleus and they have all $\Delta T = 0$, except the 0.46 → 0.13 MeV transition. The strengths yield, in combination with very conservative upper limits for M2, E3 and M3 radiation (see table 8), the restrictions on J and π as given in the last column of table 8.

Since the 0.46 MeV level has $J^\pi = 1^+$, the 2.65 → 0.46 MeV transition limits the J^π value for the 2.65 MeV level to a maximum of $3^\pm$ or 4^-. The ground-state transition of the 3.42 MeV level limits the J^π value of this level to a maximum of $5^\pm$ or 6^- and the restrictions on the 3.46 → 3.42 and 3.46 → 2.65 MeV transitions limit the J^π value of the 3.46 MeV level to a maximum of $6^\pm$ or 7^+.

These maximum J^π values are given between brackets in fig. 5. The parity of the 2.65 MeV level is taken as negative on the basis of the observation of odd l_n values in the neutron pick-up reactions ^{39}K(d, τ)^{38}K [ref. [33])] and ^{39}K(τ, α)^{38}K [ref. [34])].

It should be noted that a spin assignment of $J = 7$ to the 3.46 MeV level, in combination with the results presented in table 8, leads unambiguously to the results of π(3.46 MeV) = +, J^π(2.65 MeV) = 4^- and J^π(3.42 MeV) = 6^-.

4.4. ISOMERISM

We suggest that the occurrence of the isomeric state is due to its shell-model configuration $[(1d_{\frac{3}{2}})^4_{00}(1f_{\frac{7}{2}})^2_{70}]_{J^\pi=7^+,\,T=0}$. This configuration comes at a rather low excitation energy, such that the underlying high-spin levels have mainly the configuration $[(1d_{\frac{3}{2}})^5(1f_{\frac{7}{2}})]_{J,\,\pi=-}$. The γ-decay of the isomeric level then thas to take place via parity-changing transitions of which, in the self-conjugate ^{38}K nucleus E1 is forbidden and M2 inhibited by a factor of about 100.

The particle break-up channels ^{37}Ar+p, ^{37}K+n, ^{36}Ar+d, ^{35}Ar+t, ^{35}Cl+τ and ^{34}Cl+α are all closed by at least 1.6 MeV. Also the β^- decay channel to ^{38}Ca is closed by 3.3 MeV. The energetically possible β^+ decay to ^{38}Ar would be unobservably weak due to the relatively short lifetime.

Supporting (but not unambiguous) evidence that the isomeric state has mainly the configuration $[(1d_{\frac{3}{2}})^4_{00}(1f_{\frac{7}{2}})^2_{70}]_{J^\pi=7^+,\,T=0}$ is obtained from the following data:

(i) The result of g(3.46 MeV) = +0.548±0.002 obtained by Iordachescu *et al.* [5]) is consistent with a pure $(1f_{\frac{7}{2}})^2$ configuration with $J^\pi = 7^+$.

(ii) A deuteron spectrum of the ^{36}Ar(α, d)^{38}K reaction [6]), taken at E_α = 35 MeV and with a resolution of about 50 keV, is dominated by a state at 3445±20 keV. A spin assignment of 7^+ is made [6]) on the basis of the intensity and angular distribution of the deuteron group. However, it should be remarked that presently three ^{38}K levels are known in this excitation range namely at 3420.0±0.2, 3432±2 [ref. [35])] and 3458.0±0.2 keV.

(iii) The fact that the 3.46 MeV level is strongly populated in a heavy-ion reaction is consistent with a high spin.

(iv) A large shell-model calculation [36]) gives a preliminary result of about 3.5 MeV for the excitation energy of a pure $(1f_{\frac{7}{2}})^2$ state with $J^\pi = 7^+$, $T = 0$.

The assistance of R. L. W. van de Weg and J. Konieczek in taking and analysing data is gratefully acknowledged. This work was performed as part of the research program of the "Stichting voor Fundamenteel Onderzoek der Materie" (FOM) with financial support from the "Nederlandse Organisatie voor Zuiver Wetenschappelijk Onderzoek" (ZWO).

References

1) F. C. Erné, Nucl. Phys. **84** (1966) 91
2) B. H. Wildenthal, E. C. Halbert, J. B. McGrory and T. T. S. Kuo, Phys. Rev. **C4** (1971) 1266
3) E. A. Ivanov, A. Iordăchescu and G. Pascovici, Rev. Roumaine de Phys. **14** (1969) 317
4) H. Hasper, P. B. Smith and P. J. M. Smulders, Phys. Rev. **C5** (1972) 1261
5) A. Iordăchescu, E. A. Ivanov and G. Pascovici, Phys. Lett. **48B** (1974) 28
6) R. Kouzes and R. Sherr, Bull. Am. Phys. Soc. **18** (1973) 602, and private communication
7) P. M. Endt and C. van der Leun, Nucl. Phys. **A214** (1973) 1
8) M. A. van Driel *et al.*, Proc. Int. Conf. on nuclear physics, Munich 1973, p. 205
9) D. H. White, R. E. Birkett and T. Thomson, Nucl. Instr. **77** (1970) 261
10) G. A. P. Engelbertink and J. W. Olness, Phys. Rev. **C5** (1972) 431
11) D. C. Camp and G. L. Meredith, Nucl. Phys. **A166** (1971) 349
12) C. M. Lederer, J. M. Hollander and I. Perlman, Table of isotopes, 6th ed. (Wiley, NY, 1967)
13) Y. Gurfinkel and A. Notea, Nucl. Instr. **57** (1967) 173
14) W. R. Kane and M. A. Mariscotti, Nucl. Instr. **56** (1967) 189
15) H. Hasper and P. B. Smith, Phys. Rev. **C8** (1973) 2240
16) M. E. Rose, Internal conversion coefficients (North-Holland, Amsterdam, 1958)
17) K. W. Jones, A. Z. Schwarzschild and E. K. Warburton, Phys. Rev. **178** (1969) 1773
18) A. B. McDonald, T. K. Alexander, O. Häusser and G. T. Ewan, Can. J. Phys. **49** (1971) 2886
19) R. Engmann, E. Ehrmann, F. Brandolini and C. Signorini, Nucl. Phys. **A162** (1971) 295
20) F. Brandolini, M. de Poli and C. Rossi Alvarez, Nuovo Cim. Lett. **8** (1973) 342
21) K. P. Lieb, Köln, private communication
22) N. Anyas-Weiss *et al.*, Nucl. Phys. **A201** (1973) 513
23) R. D. Barton, J. S. Wadden, A. L. Carter and H. L. Pai, Can. J. Phys. **49** (1971) 971
24) F. Ingebretsen, T. K. Alexander, O. Häusser and D. Pelte, Can. J. Phys. **47** (1969) 1295
25) G. A. P. Engelbertink *et al.*, Phys. Lett. **33B** (1970) 353
26) B. D. Kern and P. D. Bond, Nucl. Phys. **A181** (1972) 403
27) J. Lindskog, D. M. Gordon and R. W. Kavanagh, Nucl. Phys. **A187** (1972) 1
28) G. C. Ball *et al.*, Nucl. Phys. **A182** (1972) 529
29) R. Griffiths *et al.*, Phys. Rev. **C8** (1973) 168
30) A. Gallmann, E. Aslanides, F. Jundt and E. Jacobs, Phys. Rev. **186** (1969) 1160
31) T. T. Bardin and J. A. Becker, Phys. Rev. Lett. **27** (1971) 866
32) J. D. Goss, Notre Dame, private communication
33) H. T. Fortune, N. G. Puttaswamy and J. L. Yntema, Phys. Rev. **185** (1969) 1546
34) J. A. Fenton *et al.*, Nucl. Phys. **A187** (1972) 123
35) W. K. Collins *et al.*, Bull. Am. Phys. Soc. **17** (1972) 534
36) H. Hasper, Groningen, private communication